RESEARCH PAPER

Cancer Biology & Therapy 10:1, 1-6; July 1, 2010; © 2010 Landes Bioscience

Bioluminescent imaging study

FAK inhibitor, PF-562,271, preclinical study in PC3M-luc-C6 local implant and metastasis xenograft models

Haihao Sun,[1] Stephen Pisle,[2] Erin R. Gardner[3] and William D. Figg[1,2,*]

[1]Molecular Pharmacology Section; and [2]Clinical Pharmacology Program; Medical Oncology Branch; Center for Cancer Research; National Cancer Institute; Bethesda, MD USA; [3]Clinical Pharmacology Program; SAIC-Frederick; NCI-Frederick; MD, USA

Key words: prostate cancer, in vivo, luciferase, focal adhesion kinase

Focal adhesion kinase (FAK) is essential in regulating integrin signaling pathways responsible for cell survival and proliferation, as well as motility, making FAK a distinctive target in the field of anticancer drug development, especially with regards to metastatic disease.[1] Our objective was to demonstrate tumor growth inhibition by PF-562,271, a selective inhibitor of FAK and FAK2, or Pyk2,[2] in mouse xenograft models, both subcutaneous and metastatic, employing the human prostate cancer cell line PC3M-luc-C6, a modified PC3M cell line that expresses luciferase. After two weeks of treatment with PF-562,271, 25 mg/kg PO BID 5x/wk, the subcutaneous model showed a 62% tumor growth inhibition compared to control based on tumor measurements ($p < 0.05$), with a 88% vs. a 490% increase in bioluminescent signal for treatment and control respectively ($p < 0.05$). In the metastasis model, the percent change from baseline, after 18 days of treatment, of the treatment group was 2,854% vs. 14,190% for the vehicle ($p < 0.01$). These results show that PF-562,271 has a potent effect on metastatic prostate cancer growth in vivo.

Introduction

Focal adhesion kinase (FAK) is an essential regulator of integrin signaling pathways. It plays a critical role in cell growth, in an adhesion-independent manner. The expression level of FAK is increased in most human cancers, particularly during transformation into highly invasive metastases.[3] The disruption of FAK activity and function may become a unique approach to targeted anticancer therapy against many solid tumors.[4]

PF-562,271 is an ATP-competitive reversible inhibitor of FAK developed to target tumor and endothelial cells. It was introduced as a first in class inhibitor present in clinical testing for cancer treatment. It has shown promising tumor regression effect in a variety of subcutaneously inoculated xenograft models including LoVo human colon cancer, BT-474 human breast cancer, PC-3M prostate cancer, and BxPc3 human pancreatic cancer.[2] However, it has never been tested in any mouse xenograft models of metastasis. PC3M-luc-C6 cells, derived from metastasized lesions of human prostate adenocarcinoma cells PC3M, modified to express luciferase, can be used in a metastasis xenograft model to monitor treatment response non-invasively.[5] Although it initially responds well to hormonal and surgical therapies, prostate cancer eventually progresses to castrate resistance and metastasizes to the bone in most cases.[6] Despite research efforts in seeking an effective cure for this condition, there is no established efficacious treatment for castrate resistant prostate cancer (CRPC) and bone metastasis.

In order to ascertain disease progression in a metastatic disease model, bioluminescent imaging is frequently employed. Bioluminescent imaging (BLI) displays images based upon the visible light emission from bioluminescent firefly luciferase expressing cells. It has been applied in monitoring gene expression, therapeutic response and protein-protein interaction in both in vitro and in vivo models.[8-11] BLI provides a sensitive, rapid, non-invasive and cost-effective method to conduct drug efficacy studies in the preclinical xenograft animal model, especially a metastasis model, by measuring the change in luciferase expression.[12] Previous studies in mouse models with PF562,271 have not employed bioluminescent imaging techniques. Therefore, we conducted the current study to further explore the effect of this drug in both PC3M-luc-C6 subcutaneous local implant and metastasis xenograft models.

Results

Efficacy study in subcutaneously inoculated xenograft model. Tumor growth retardation was observed in the PF-562,271 treatment group in comparison with vehicle control, as shown in **Figure 1**. The percent increase in tumor size of the vehicle control group and drug treatment group was statistically significant ($p < 0.05$) starting at day seven, 5% (±18) for treatment versus 45% (±12) for vehicle, to the end of the treatment (day 14), 40% (±47) treated versus 110% (±19) control. Percent growth inhibition was

*Correspondence to: William D. Figg; Email: wdfigg@helix.nih.gov
Submitted: 08/28/09; Revised: 03/10/10; Accepted: 04/09/10
Previously published online: www.landesbioscience.com/journals/cbt/article/11993

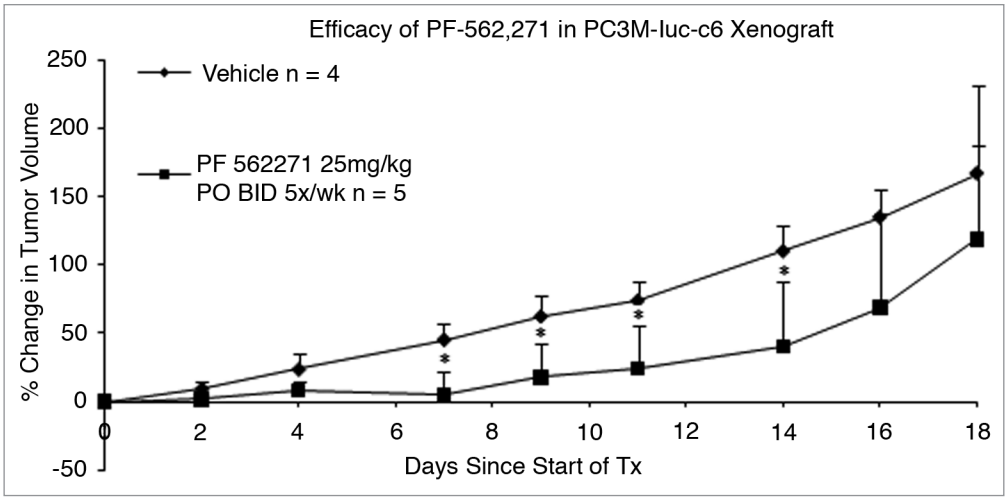

Figure 1. Efficacy of PF-562,271 in PC3M-luc-C6 subcutaneuous local implant xenograft model: PF-562,271 was administered at 25 mg/kg P.O. BID 5x/wk for two weeks. Tumor volumes measured on day 0, prior to the treatment, were used as a baseline. Percent Change in tumor volume = 100 * $\sum[(x_i - x_{i(0)})/x_{i(0)}]/n$. Error bars represent standard deviation. *indicates a p-value <0.05.

62% on day 14. Statistical difference between vehicle control and treatment groups did not persist after the end of treatment. No weight loss or other morbidity was observed in either group during the treatment period. No deaths occurred in the vehicle group, but two mice in the treatment group were euthanized at days 16 and 18 due to tumor ulceration.

Bioluminescent imaging study in subcutaneously inoculated xenograft model. The mice of both vehicle control and drug treatment groups of the efficacy study were imaged 3 days prior to the initiation of the treatment and photon intensities of tumor ROIs were used as the baseline. Percent change in photon intensity relative to the baseline was used to quantify changes in cellular activity. The difference in photon intensity ratio (as shown in **Fig. 2**) was statistically significant ($p < 0.05$) only on day 11, 88% (±49) vs. 490% (±199), treated and control respectively. Data for day 14 was not significant due to a reduction in signal in the vehicle control group, most likely because of tumor necrosis. A series of representative images from vehicle control group and PF-562,271 treatment group are shown in **Figure 3**. The signal intensity of tumor from vehicle mouse dramatically increased with time, whereas it showed only slight enhancement in treated mice.

BLI study in intra-cardiac inoculated metastasis xenograft model. Since there were multiple detectable lesions observed in the dorsal image of each mouse, those lesions were followed up and analyzed separately over time. A series of representative follow-up images from vehicle control group and PF-562,271 treatment group are shown in **Figure 4**. The data derived from one representative lesion per mouse and average signal of multiple lesions per mouse are shown in **Figure 5**. There was insufficient data for day 24 due to a death in the vehicle control group. The average percent change from baseline for vehicle control and treated group are 13,520% and 2,938% respectively ($p = 0.07$), based upon analysis of the largest lesion per mouse on day 18. Based upon analysis of the average signal for multiple lesions per mouse on day 18, the average percent change for vehicle control and treated group are 14,190% and 2,854% respectively ($p = 0.006$).

The mice used in the metastasis model were also imaged on the ventral side (data not shown), but the difference between the groups did not reach significance due to saturation of the detector at later time points for both the vehicle and treatment groups. The cause of this is the placement of the lesions which, upon post-study necropsy, were evident only on the ventral area. Lesions were visible in the ribs and sternum, with some lesions having extended out of the bone into surrounding tissues. While some lesions were found in the abdomen, the majority of the lesions were found in bones. No lesions were evident in the lungs or heart, though one mouse had a small lesion on the liver while the main lesion of another mouse, in the treatment group, was intramuscular. Mice that died during the study were not examined by necropsy, though imaging did show the presence of at least one mandibular lesion and abdominal lesions.

Discussion

FAK inhibitor PF-562,271 has shown marked tumor suppression effect in both local implant and metastasis xenograft models employing PC3M-luc-C6. It was well tolerated by the mice in this study. There was no weight loss or drug induced death observed with the dosage of 25 mg/kg P.O. BID 5x/wk used in this study. This is consistent with the findings observed in the previous studies using different tumor xenograft models.[2]

Since most metastasis of prostate cancer occurs in the bone, it is essential to establish a comparable bone metastasis model to conduct preclinical trials in the effort of mimicking clinical condition and seeking treatment for the condition. Intra-cardiac inoculation has been proven effective in generating an in vivo metastasis model that can result in lesions in both the lymph nodes as well as in bone.[5] Using this method, we have established a wide-spread prostate cancer metastasis model based upon necropsy confirmation.

BLI study reveals the level of luciferase expression and reflects the level of cellular activity at the time of imaging. It is comparable

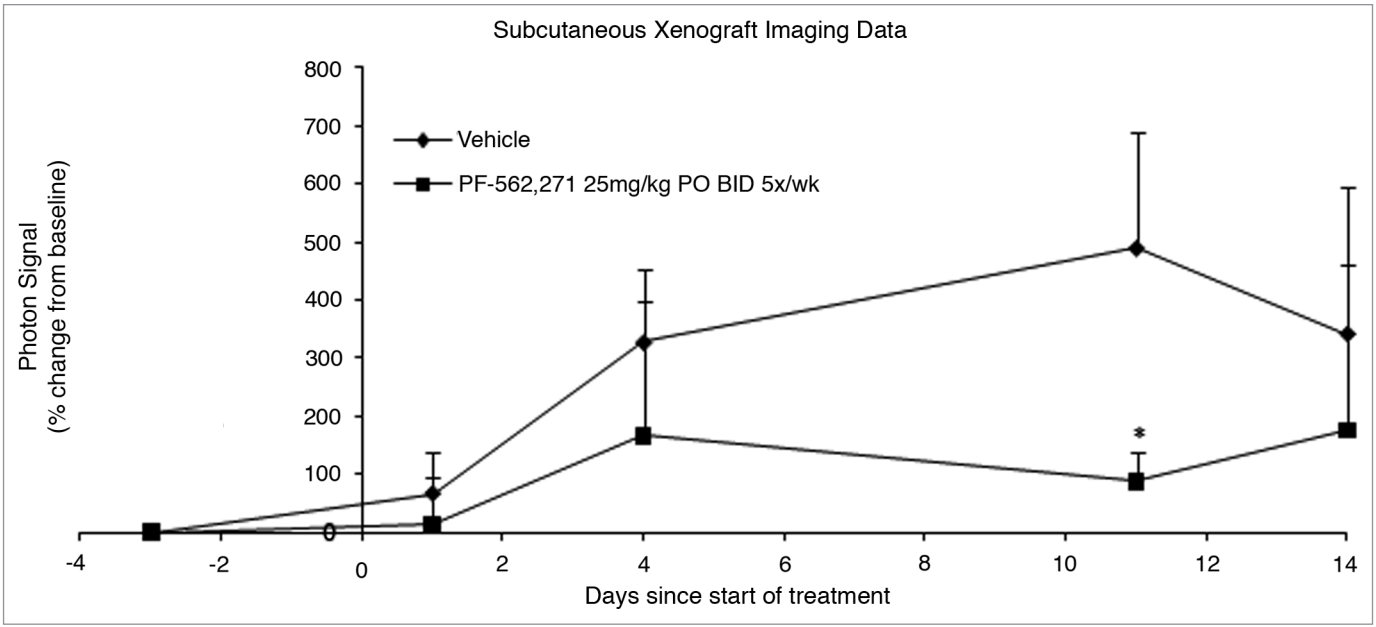

Figure 2. ROI photon intensity time course of the BLI study from subcutaneous local implant xenograft model: PF-562,271 was administered at 25 mg/kg P.O. BID 5x/wk for two weeks. One mouse from each group was excluded due to a large initial tumor size. Percent Change in tumor signal = 100 * $\sum[(x_i - x_{i(0)})/x_{i(0)}]/n$. Error bars represent standard deviation. The difference between treatment and vehicle control is significant on day 11. Tumor necrosis in the vehicle control is the most likely cause for degradation of signal on day 14. * indicates a p-value <0.05.

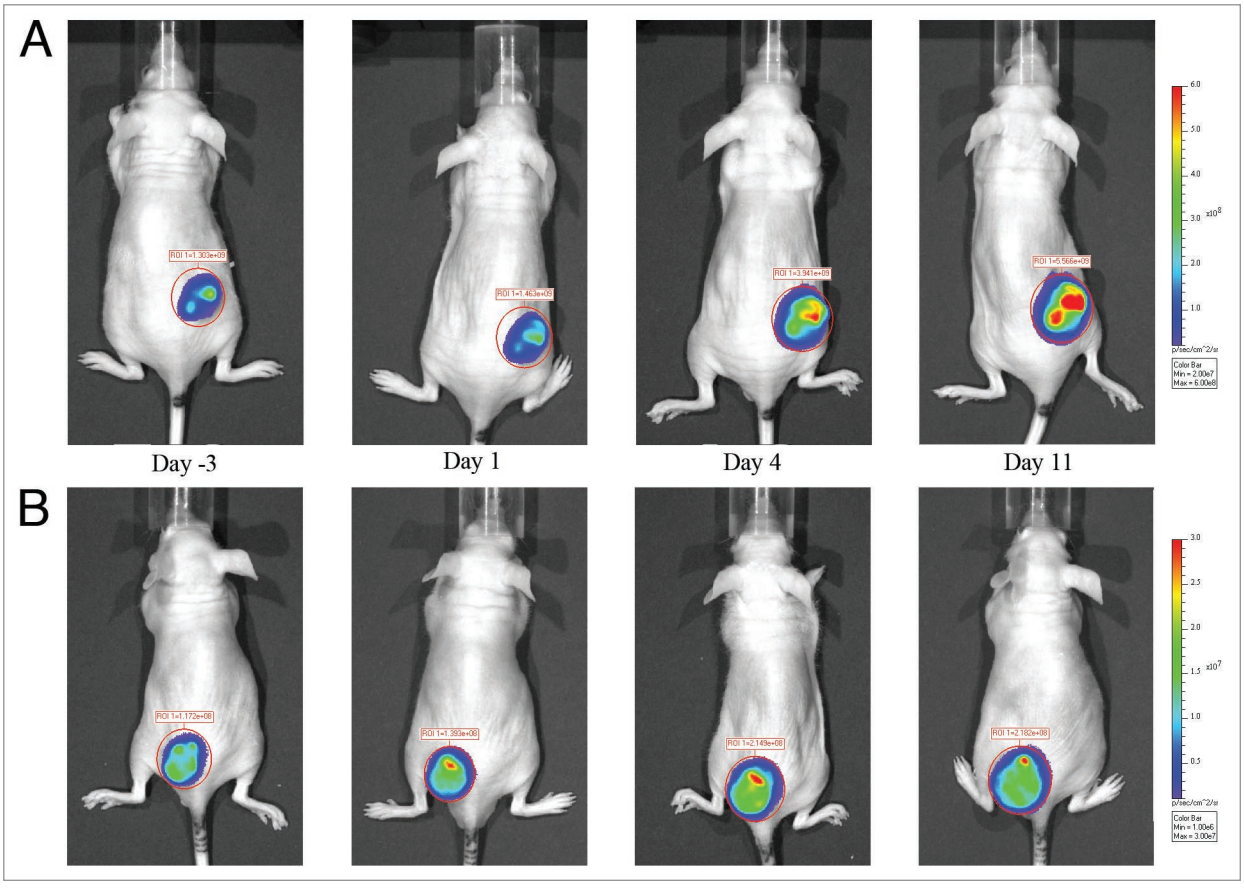

Figure 3. (A) Bioluminescent image time course of a subcutaneously inoculated vehicle control mouse. PF-562,271 was administered at 25 mg/kg P.O. BID 5x/wk for two weeks. (B) Bioluminescent image time course of a subcutaneously inoculated mouse treated with PF-562,271. PF-562,271 was administered at 25 mg/kg P.O. BID 5x/wk for two weeks.

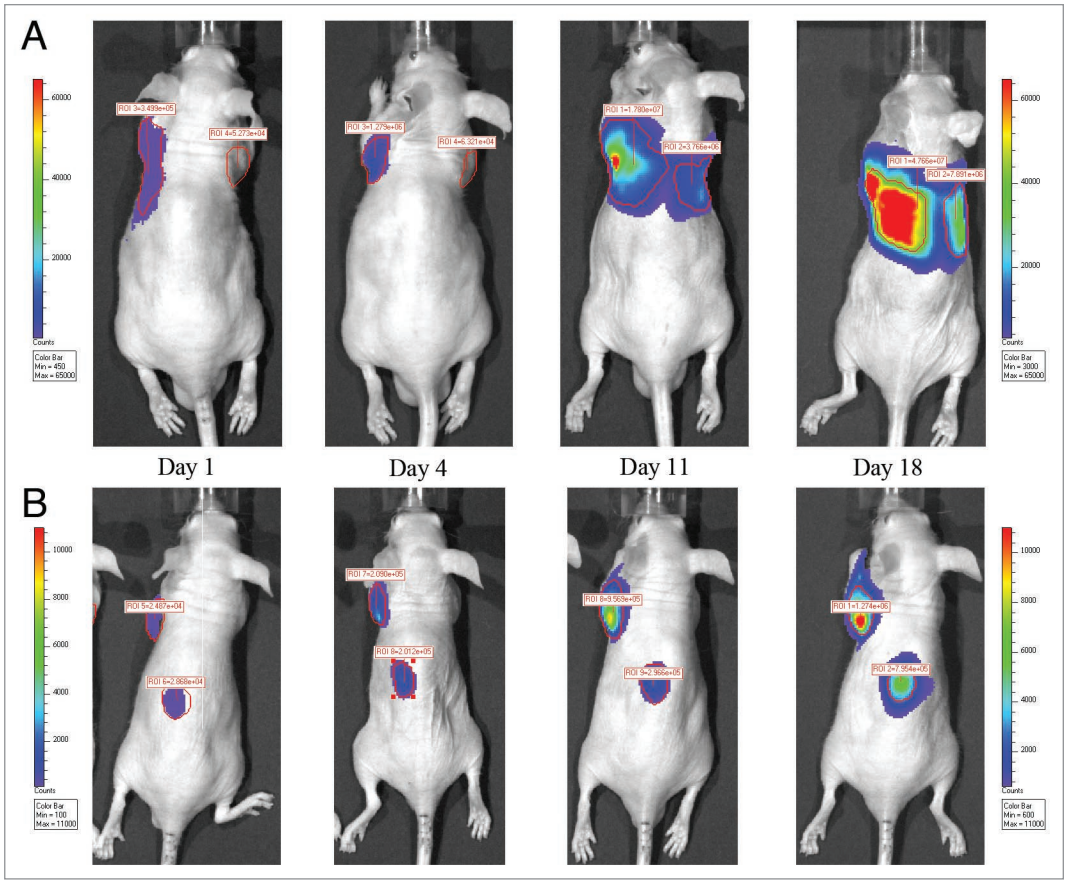

Figure 4. (A) Bioluminescent image time course of an intracardiac inoculated vehicle control mouse. Vehicle was administered P.O. BID 5x/wk for three weeks. (B) Bioluminescent image time course of an intracardiac inoculated treated with PF-562,271. PF-562,271 was administered at 25 mg/kg P.O. BID 5x/wk for three weeks.

though different from imaging methods as micro-CT, micro-PET and MRI that detect anatomic alteration to monitor the tumor response to treatment, with the added benefit that micro-metastases can be directly measured in a rapid, high throughput environment.[13] There was a clear difference in signal seen in larger tumors compared to smaller ones, even through multiple layers of tissue starting from the third day post treatment in our study. Previous in vivo studies have shown a linear relationship between tumor weight and bioluminescent signal over a large range of tumor weights for tumors in control, treatment and relapse groups for the PC3M-luc-C6 cell line.[5]

A previous study, utilizing X-ray imaging for monitoring progression, employed intratibial growth of tumors in a rat xenograft model. This study showed evidence of tumor growth suppression and bone growth upon treatment with PF-562,271, but was not able to quantify tumor growth with this method.[7]

Bone metastasis is common in breast, lung, kidney and prostate cancer. While the bone metastasis from breast, lung and kidney is osteolytic, prostate cancer bone metastasis is osteoblastic. The pattern of bone involvement from prostate cancer cells is somewhat predictable, usually starting from the axial skeleton and subsequently spreading to the appendicular skeleton. Bone overgrowth can replace hematopoietic tissue in the bone marrow and result in anemia and susceptibility to infection. It can also lead to pain, fracture and symptoms of spinal-cord compression. A previous study has demonstrated that PF-562271 has positive effects on lytic bone tumors. The authors employed intra-tibial inoculation of the MDA-MB-231 breast carcinoma cell line in a rat xenograft model.[7] Our current study has shown that PF-562,271 is efficacious in PC-3M-luc-C6, which has high expression levels of both FAK and PyK2. Positive correlation between PF-562271 efficacy and expression level of FAK and PyK2 has not been established and requires further study.

Roberts et al. have shown in a PC3M subcutaneous xenograft model that there was only 27% inhibition (ns) of phosphorylated-FAK (p-FAK) at the dose tested in our study. However, the number of apoptotic bodies increased significantly and there was a significant reduction in tumor growth.[2] Another study has shown that p-FAK staining is much higher in tumors following treatment with PF-562271.[14] Even though this is the case, it has been shown that a small degree of inhibition is sufficient to cause cessation of tumor growth, and in some cases even regression, in a variety of subcutaneous xenograft models.[2] This suggests that cells able to increase expression of FAK and/or p-FAK stability have a decreased chance of apoptosis when subjected to this therapy, leaving behind a smaller, but more highly p-FAK expressing, population of cells. A small decrease in FAK signaling has significant effects on tumor progression most likely because the FAK

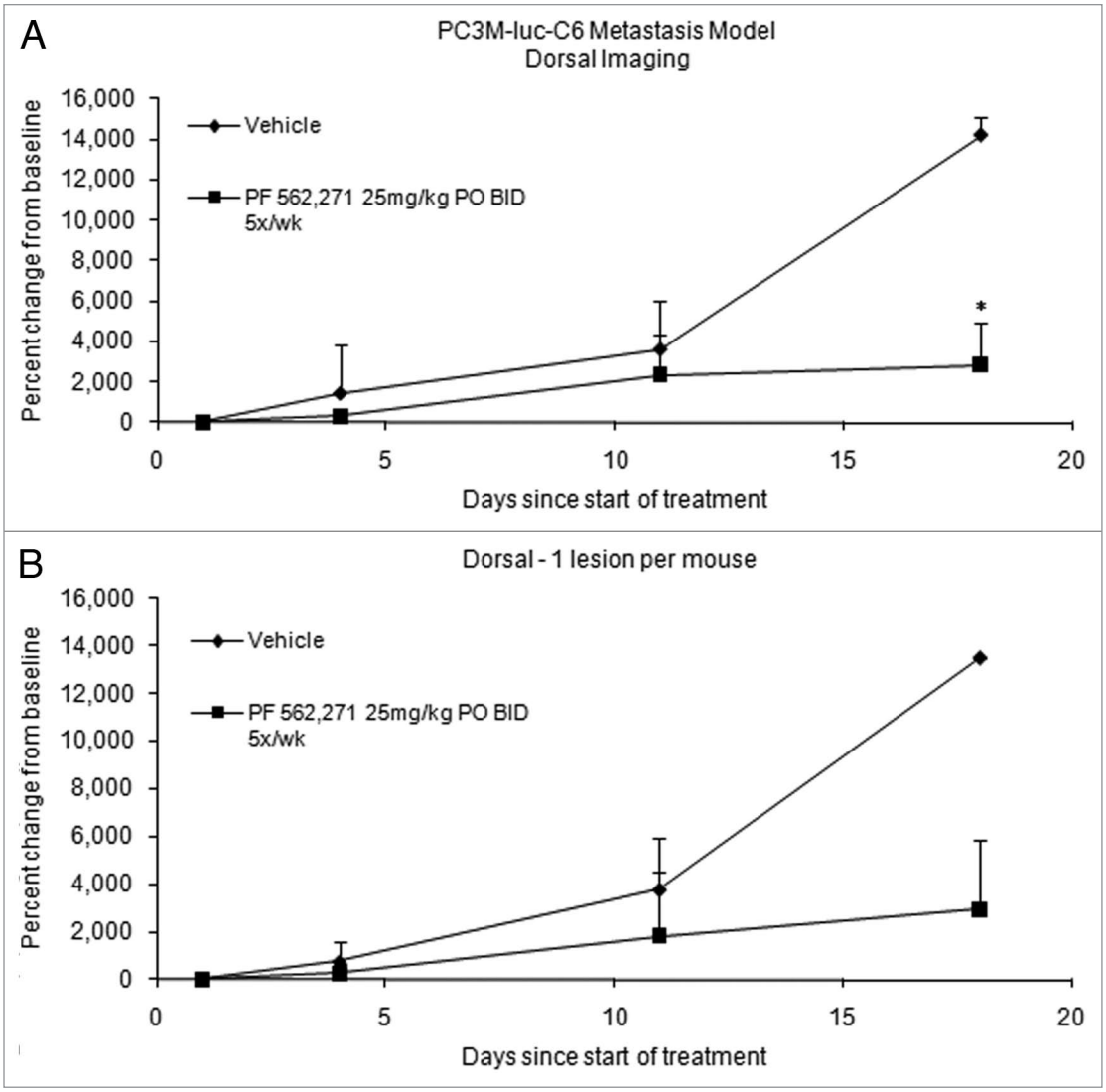

Figure 5. ROI photon intensity time course of the BLI study from metastasis xenograft model: The ROI was drawn on the dorsal images. Percent change, based on baseline (day 1), in a metastatic prostate cancer model treated with PF 562271 (n = 3) vs. Vehicle control (n = 3). Of the 5 original mice in each group, 2 mice were excluded from each due to lack signal from the dorsal face at baseline; data is only complete up to day 18 due to these exclusions. Percent Change in tumor signal = 100 * $\sum[(x_i - x_{i(0)})/x_{i(0)}]/n$. Error bars represent standard deviation. PF-562,271 was administered at 25 mg/kg P.O. BID 5x/wk for three weeks. * indicates a p-value <0.05. (A) Multiple lesions were imaged in at least one mouse from each group. The difference between vehicle and treatment was significant ($p < 0.01$) by two tailed t-test for day 18. (B) When only the largest lesion per animal is measured, the difference is not significant due to low sample number.

family of signaling molecules is involved in multiple signaling pathways important in cell growth and motility, many of which have been targeted with other agents.

A previous study has shown that microvessel counts decreased upon PF-562271 treatment indicating that this drug has an anti-angiogenic effect.[2] It has been well recognized that angiogenesis plays a crucial role in promoting metastasis in prostate cancer.[15] As such, the anti-tumor activity of PF-562271 observed in our current prostate cancer bone metastasis xenograft model might be due to an antiangiogenic effect.

In conclusion, our current study confirmed the findings that PF-562271 is well tolerated and efficacious in preclinical study with the current regimen. Treatment with PF-562271 caused a significant decrease in tumor progression in both subcutaneous and bone metastasis PC3M-luc-C6 xenograft models and was successfully detected with bioluminescent imaging in both models.

Methods and Materials

Drugs. PF-562,271 was kindly provided by Pfizer, Inc., (Groton, Connecticut). The stock solution (12.5 mg/ml) was made by dissolving the drug in a solution of 50% DMSO (Sigma), 50% PEG-400 (Sigma), and stored at -20°C. Aliquots of the stock solution were diluted in sterile saline to the final dosing concentration immediately prior to treatment.

Animals. Male BALB/cAnNCr-nu/nu mice were obtained from the NCI-Frederick Animal Production Area (Frederick, MD, USA). The National Cancer Institute is accredited by AAALAC International and follows the Public Health Service Policy for the Care and Use of Laboratory Animals. Animal care was provided in accordance with the procedures outlined in the "Guide for Care and Use of Laboratory Animals" (National Research Council; 1996; National Academy Press; Washington, DC). The study protocol was approved by the NCI Animal Care and Use Committee (Bethesda, MD).

Tumor inoculation and monitoring. *Local implant model.* PC-3M-Luc-C6 cells were obtained from Xenogen, Corp., (Cranbury, NJ). The cell line was PCR tested negative for more than 18 mouse pathogens to ensure sterility (MU research animal diagnostic laboratory, Columbia, MO65211) and cultured according to supplier instructions. Once 80% confluence was reached, cells were harvested, washed and diluted with sterile PBS buffer. One million cells were injected subcutaneously, in a total volume of 100 µl, into the rear flank of each mouse using a 27 ga needle. Mice were monitored and weighed 3 times per week. Once the tumors become palpable, mice were randomized to one of the following two treatment groups:

(1) Vehicle group: 4 mice, 6 ml/kg, PO, BID, 5x/wk for 2 weeks

(2) PF562271 group: 5 mice, 25 mg/kg, PO, BID, 5x/wk for 2 weeks.

Tumor measurements were performed 3 times per week with digital calipers. Volume was calculated by $V = \pi/6 * l * w * h$. Imaging was performed 3 days before the start of treatment and on days 1, 4, 11 and 14 after the start of treatment.

Metastasis model. The mice were placed on the surgical table and the limbs were securely taped to prevent potential movements under general anesthesia of inhaled isoflurane. 5×10^5 PC3M-luc-C6 cells were injected into the left ventricle of each mouse by inserting the needle into the 2nd intercostal space next to the sternum. The mice were imaged before the inoculation and every other day after the inoculation to monitor the tumor progression. Once sufficient visible signals were obtained, the mice were randomized into vehicle control (n = 5) and treatment (n = 5) groups similar as described above, but with treatment lasting for 3 weeks. The bioluminescent images were obtained at day 0 prior to the initiation of the treatment as well as day 1, 4, 11, 18 and 24 during the treatment. Necropsy was performed on mice surviving for two weeks after the completion of treatment to confirm the location of imaged lesions.

Statistical analysis. The data of the tumor progression and regression, represented as the percent change from baseline for each individual animal, was analyzed by one-way ANOVA for statistical comparison. Individual groups were compared by t-test. A p-value of less than 0.05 was considered to be significant.

Bioluminescent imaging study. The mice were imaged prior to treatment and weekly during the treatment using a Xenogen Lumina bioluminescent imager, with data analysis performed using Xenogen living imaging software (V. 2.50). Mice were injected with D-Luciferin Firefly, potassium salt (Biosynth, Inc.,) 150 mg/kg I.P. shortly before imaging. The region of interest (ROI) was defined over the contour of each individual tumor to include all photon emission from the entire tumor. All images were formatted with the same color coded scale for visual assessment. The average percent change of the photon intensity of all ROIs in each group was used to demonstrate the change in cellular activities of the tumor cells during the course of the treatment.

Acknowledgements

This project has been funded in whole or in part with federal funds from the National Cancer Institute, National Institutes of Health, under contract HHSN261200800001E (E.R.G.). This work was supported by the Intramural Research Program of the NIH, National Cancer Institute, Center for Cancer Research.

Disclaimer

The content of this publication does not necessarily reflect the views or policies of the Department of Health and Human Services, nor does mention of trade names, commercial products, or organization imply endorsement by the U.S. Government.

References

1. Johnson TR, Khandrika L, Kumar B, Venezia S, Koul S, Chandhoke R, et al. "Focal Adhesion Kinase Controls Aggressive Phenotype of Androgen-Independent Prostate Cancer." Mol Cancer Res 2008; 6:1639-48.
2. Roberts WG, Ung E, Whalen P, Cooper B, Hulford C, Autry C, et al. "Antitumor activity and pharmacology of a selective focal adhesion kinase inhibitor, PF-562,271." Cancer Res 2008; 68:1935-44.
3. Gabarra-Niecko V, Schaller MD, Dunty JM. FAK regulates biological processes important for the pathogenesis of cancer. Cancer Metastasis Rev 2003; 22:359-74.
4. McLean GW, Carragher NO, Avizienyte E, Evans J, Brunton VG, Frame MC. The role of focal adhesion kinase in cancer—a new therapeutic opportunity. Na Rev Cancer 2005; 5:505-15.
5. Jenkins DE, Yu SF, Hornig YS, Purchio T, Contag PR. "In vivo monitoring of tumor relapse and metastasis using bioluminescent PC-3M-luc-C6 cells in murine models of human prostate cancer." Clin Exp Metastasis 2003; 20:745-56.
6. Loberg RD, Logothetis CJ, Keller ET, Pienta KJ. "Pathogenesis and Treatment of Prostate Cancer Bone Metastases: Targeting the Lethal Phenotype." J Clin Oncol 2005; 23:8232-41.
7. Bagi CM, Roberts WG, Andresen CJ. "Dual focal adhesion kinase/Pyk2 inhibitor has positive effects on bone tumors: implications for bone metastases." Cancer 2008; 112:2313-21.
8. Contag CH, Jenkins D, Contag PR, Negrin RS. "Use of reporter genes for optical measurements of neoplastic disease in vivo." Neoplasia 2000; 2:41-52.
9. Contag PR, Olomu IN, Stevenson DK, Contag CH. "Bioluminescent indicators in living mammals." Nat Med 4:245-7.
10. Honigman A, Zeira E, Ohana P, Abramovitz R, Tavor E, Galun E, et al. "Imaging transgene expression in live animals." Mol Ther 2001; 4:239-49.
11. Carlsen H, Moskaug JØ, Fromm SH, Blomhoff R. "In vivo imaging of NFkappaB activity." J Immunol 2002; 168:1441-6.
12. Zhang Y, Bressler JP, Neal J, Lal B, Bhang HE, Laterra J, Pomper MG. ABCG2/BCRP expression modulates D-Luciferin based bioluminescence imaging. Cancer Res 2007; 67:9389-97.
13. Hollingshead MG, Bonomi CA, Borgel SD, Carter JP, Shoemaker R, Melillo G, Sausville EA. "A potential role for imaging technology in anticancer efficacy evaluations." Eur J Cancer 2004; 40:890-8.
14. Bagi CM, Christensen J, Cohen DP, Roberts WG, Wilkie D, Swanson T, et al. "Sunitinib and PF-562,271 (FAK/Pyk2 inhibitor) effectively block growth and recovery of human hepatocellular carcinoma in a rat xenograft model." Cancer Biol Ther 2009; 8:856-65.
15. Zetter BR. "Angiogenesis and Tumor Metastasis." Ann Rev Med 1998; 49:407-24.